Combined effects of thin-section size, grain size and cavities on the high temperature creep fracture properties of a nickel-base superalloy

A. BALDAN*
Department of Mechanical Engineering, Eastern Mediterranean University, G. Magosa, Mersin 10, Turkey

The creep fracture characteristics of a conventionally cast (CC) MAR-M 002 superalloy, controlled by the grain-boundary diffusion mechanism, have been investigated at various specimen section-sizes D, and grain sizes, d. It is observed that the creep rupture strain (or ductility), ε_R, is controlled by the $D^2/(n_G l)$ ratio, where n_G is the number of grains per cross-section of specimen and l is the half-cavity spacing, at the creep conditions (900 °C/300 MPa). A rapid improvement in creep rupture life can be made by reducing the $(d_C/d)/D$ ratio [or, equivalently, the $(d_C n_G)/D^2$ ratio] below a critical value ($\sim 100 \times 10^{-8}$ μm^{-1}), where d_C is the cavity size. The thin-section size dependent creep rupture life, t_R/D, and creep rupture strain, ε_R/D, are explained on the basis of grain boundary sliding (GBS) and creep crack growth (CCG) behaviour of the alloy. ε_R/D and t_R/D can be improved by reducing the GBS rate. A large improvement in t_R/D can be achieved by reducing the GBS and CCG rates below the critical values of these rates by reducing the crack size through increasing the grain size above a critical value. (Above a critical grain size value the crack size becomes so small that, as a result, a large increment of t_R is achieved.)

1. Introduction

The creep properties of nickel-base superalloy materials are sensitive to section size and tend to decrease with reducing cross-section of material. Small air-cooled aero engine blades have thin regions in the cross-section of the aerofoil, but thin-section CCs have much reduced creep rupture lives compared with their thick section counterparts [1–3]; for example, at a section thickness of 1 mm CC blade alloys may have a creep life that is only 20% of the rupture life at thick sections [4]. This effect has also been found in wrought [1] and directionally solidified [5], as well as in dispersion-strengthened Ni–Cr sheets [6]. It was shown experimentally [1] on simple Ni–Cr cast and wrought alloys that the creep rupture life decreased as a result of the reduced number of grains, n_G, in the cross-section of the specimens. This reduced number of grains promoted grain boundary sliding (GBS) [7], and put a higher stress on a few randomly orientated grains. Therefore, previous works suggest that the reduction in the number of grains in the cross-section is the critical parameter [1, 2, 7].

Gas turbine blades exhibit a wide range of thicknesses due to their tapered form and the incorporation of cooling passages within the section. As mentioned above, it is known that variation of the thin-section size can lead to a change in creep properties. Furthermore, microstructural parameters are also known to affect the creep behaviour of the alloys. Therefore, the objective of this study is to ascertain the combined effects of microstructure, i.e. grain size, carbide, cavitation, etc., and thin-section size on the creep strength of a relatively complex alloy, the CC MAR-M 002 superalloy; because, according to the author's knowledge, there is not much work on this industrially important subject.

2. Experimental procedure

In this study CC MAR-M 002 is used. The bulk composition of this alloy (wt. %) is: 9.0 Cr, 10 Co, 10 W, 2.5 Ta, 5.5 Al, 1.5 Ti, 0.015 B, 0.06 Zr, 0.15 C, 1.5 Hf and balance nickel. In order to produce a variety of microstructural distributions, including grain morphology and carbide dispersion, the creep specimens were deliberately cast to shape at different solidification rates. After casting, the creep specimens were machined to various gauge diameters, D (between ~ 1.1 and 4 mm). Creep testing was carried out to failure at 1173 K (900 °C) using a uniaxial constant load in air, and the initial stress was 300 MPa. The variation of temperature with testing time was kept constant to within ± 0.5 K. Elongation of creep was recorded continuously using differential transformers. The grain size, d, of the specimen was measured, using all the grains in the grip sections, by the linear intercept method (Heyn's method): $d = (P/n'_G)$, where P is the total length of lines used and n'_G is the number of

*Address for correspondence: Dr A. Baldan, P.O. Box 348, G. Magosa, Mersin 10, Turkey.

0022–2461

grains crossed through by the lines. For the carbide dispersion measurements, from grip sections of the specimen, scanning electron microscopy (SEM) and the Cambridge Instrument Q-520 system were used for qualitative and quantitative measurements. For the cavity measurements, on the other hand, SEM cavity micrographs taken from the entire cross-sections of the fractured specimens were used for the quantitative evaluations by the Cambridge Instrument.

3. Results

3.1. Microstructure

Fig. 1 illustrates typical grain morphologies from two different specimens with different casting conditions. These micrographs indicate the wide distributions of shape and size of the grain morphologies produced as a result of different casting conditions. The measurements show that the grain sizes vary between ~ 500– ~ 1000 μm for different specimens at varying casting conditions. Typical cavity morphologies produced after the failure of creep are shown in Fig. 2. These morphologies (shapes, sizes, locations) characterize two types of cavities. As seen in Fig. 2a the cavities exist as round shapes on the grain boundary carbide particles, and are also associated with degenerate rosette type γ/γ'-eutectic pools. The morphology of the second type of cavitation is mainly continuous and massive, and is associated with eutectic pools (Fig. 2b). Fig. 2c shows the relationships between grain size, d, and cavity density, N_C for the two types of cavitation; in curve A there is a nearly linear correlation between the N_C and d, whereas in curve B, N_C is independent of d. This duel correlation between N_C and d supports the microstructural observation of cavities. Furthermore, this figure also suggests an existence of a critical grain size below which the cavity growth rate is much higher.

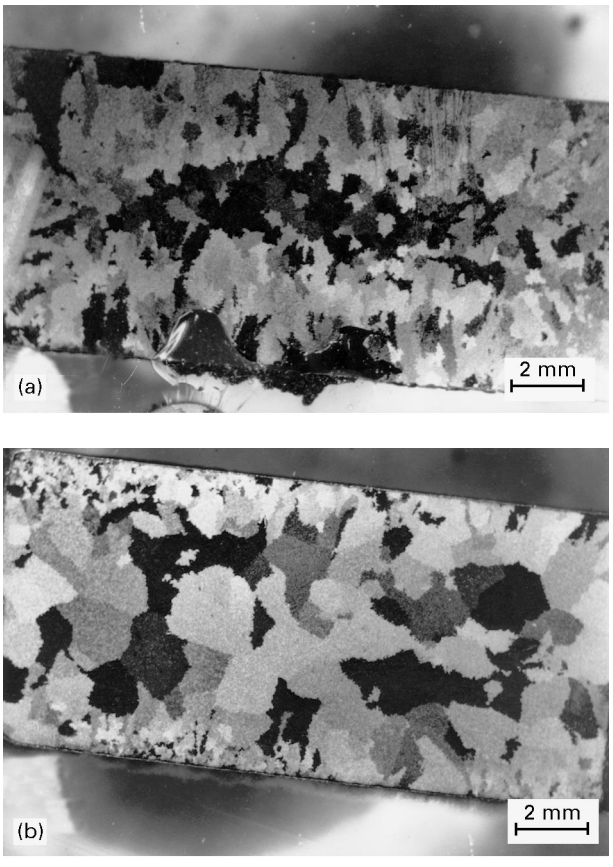

Figure 1 Typical grain morphologies from two different specimens at varying casting conditions: (a) small grain morphology, and (b) large grain structure.

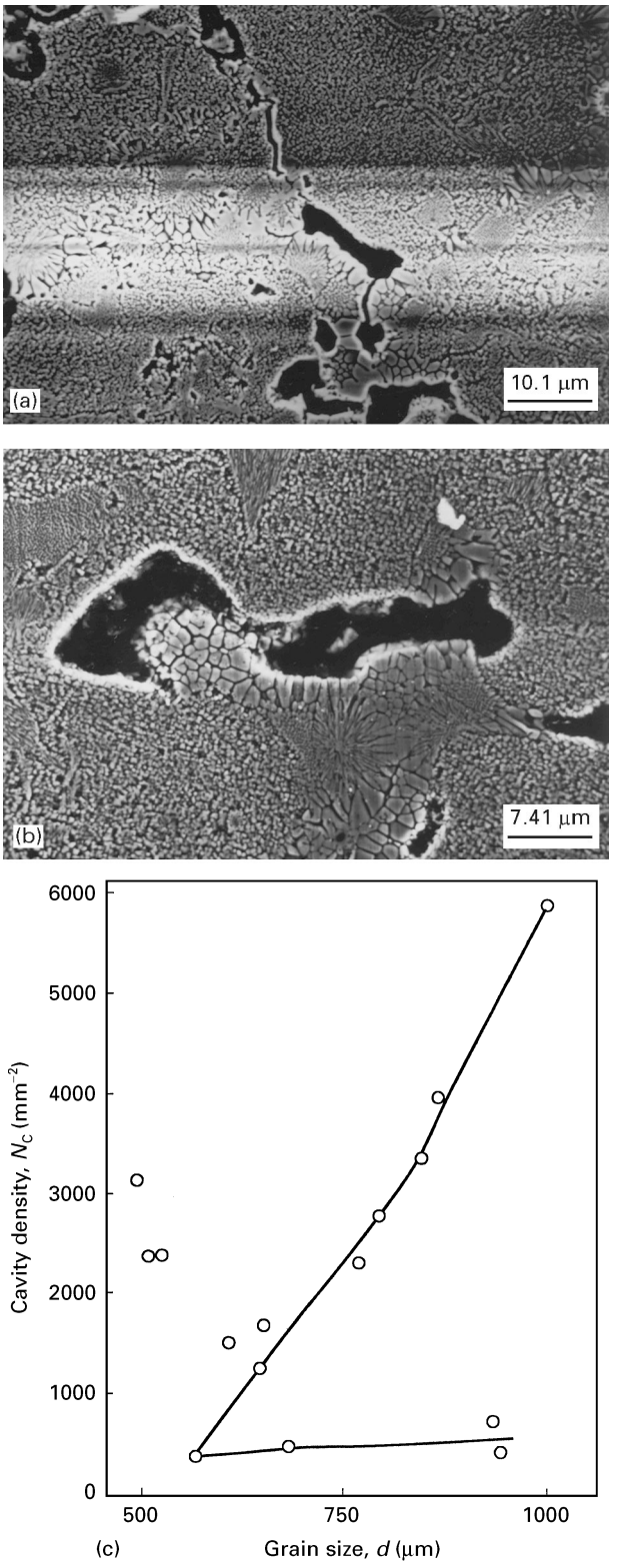

Figure 2 Two types of typical cavity morphologies observed in the creep fractured specimens: (a) discrete and elongated cavities along the serrated grain boundaries; (b) massive cavitation in the vicinity of $(\gamma + \gamma')$ eutectic pools; and (c) graph showing the two types of cavitation as functions of grain size, and indicating a critical grain size below which the cavity growth rate is appreciably higher.

3.2. Creep fracture

Fig. 3 shows the effect of the section-size, D, on the creep rupture strain, ε_R, which seems to indicate that there is a tendency for ε_R to improve with increasing section size, though there are rather large scatter in the data. This scatter in the ε_R versus D plot underlines the fact that the gauge diameter, D, of specimen is not the only dominant factor controlling the creep rupture strain.

For the grain-boundary diffusion mechanism, which is the operative creep mechanism (or cavity growth mechanism) predicted in Section 4.1. at the present creep conditions, the following relation exists between the creep rupture strain, ε_R, and the l/d ratio [8], where l is the half-cavity spacing ($L = 2l$) and d is the grain size

$$\varepsilon_R \propto (l/d) \tag{1}$$

Equation 1 indicates that the creep rupture strain is proportional to the ratio of the half-cavity spacing to grain size for the grain-boundary (GB) diffusion mechanism when the specimen section-size is "normal" (or thick). However, in the present study not only the microstructure but also the gauge diameters of the specimens were varied in order to evaluate the combined effects of thin-section size and microstructure on the creep strength of the alloy. Therefore, to include the thin-section size effect on the creep rupture strain the ratio of ε_R/D, normalizing the strain by the diameter of the testpiece, was established, because there is a tendency for the creep rupture strain to improve with increasing section size (i.e. Fig. 3), and the normalized creep rupture strain, ε_R/D, was plotted against the l/d ratio, as shown in Fig. 4. As this figure indicates there is an inverse linear correlation between ε_R/D and l/d; reducing in the l/d ratio, i.e. increasing the grain size and decreasing the cavity spacing, improves the normalized creep rupture ductility, ε_R/D. Fig. 4 therefore gives the following correlation

$$\varepsilon_R/D \propto (l/d)^{-1}$$

or rearranging this correlation and multiplying both sides of it by D gives

$$\varepsilon_R \propto (Dd/l)(D/D)$$

Assuming $D/d = n_G$ (the number of grains per gauge cross-section of specimen) yields

$$\varepsilon_R \propto D^2/(n_G l) \tag{2}$$

Equation 2 indicates that the creep rupture ductility, ε_R, improves by increasing the diameter of the testpiece and decreasing the number of grains, n_G, in the gauge cross-section. The plot of ε_R/D against n_G, as seen in Fig. 5, confirms the effect of n_G on ε_R, in which the normalized creep rupture strain, ε_R/D, value increases rapidly with the reducing number of grains. Furthermore, this plot seems to suggest that when the testpiece approaches the single crystal condition, i.e. $n_G = 1$, the ε_R/D value approaches a very high value; the scatter in this plot confirms the fact that the number of grains is not the only factor controlling the creep rupture ductility.

To show the combined effects of the testpiece diameter, D, number of grains, n_G, in the gauge section and half-cavity size, l, creep rupture ductility, ε_R, is plotted against the $D^2/(n_G l)$ ratio, according to the Equation 2, as seen in Fig. 6. This plot gives a good correlation, in which the creep rupture ductility improves rapidly with increasing $D^2/(n_G l)$ ratio up to a limiting value; further increasing this ratio does not improve ε_R. In conclusion, a large cross-sectional area, i.e. D^2, leads to a higher creep rupture ductility as a consequence of the thin-section size effect, whereas the number of grains, n_G, determines the number of grain boundaries meeting the surface of the specimen. Therefore, the number of grains has a detrimental

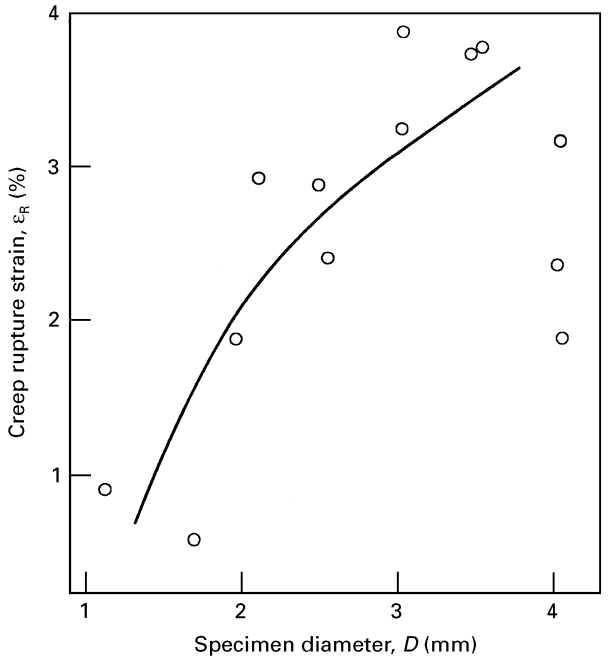

Figure 3 Effect of specimen section-size on the creep rupture strain, ε_R.

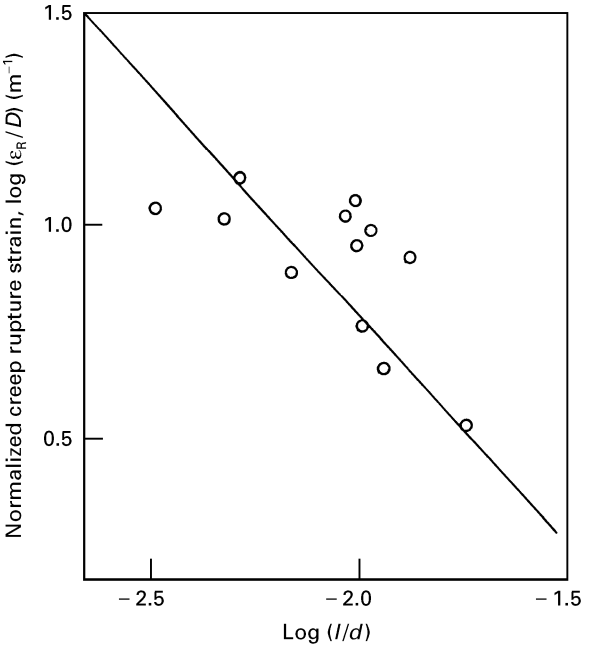

Figure 4 Showing the linear correlation between the normalized creep rupture strain, ε_R/D, and the half-cavity size to grain size ratio, l/d.

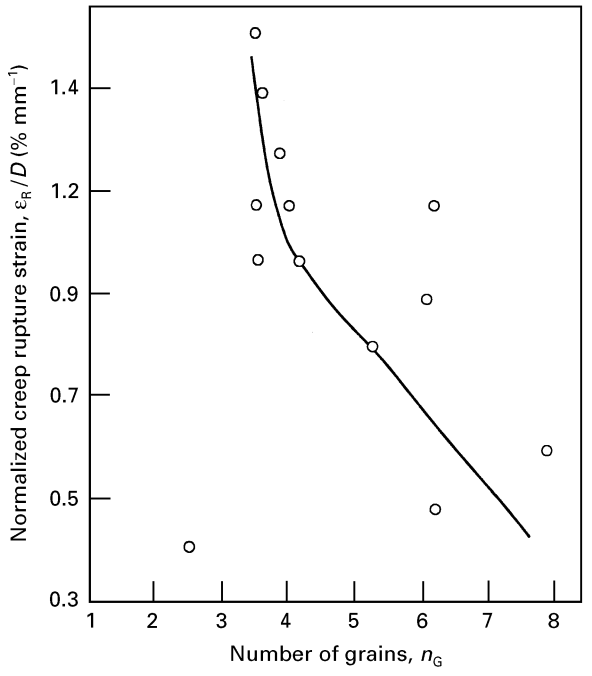

Figure 5 Effect of number of grains, n_G, per cross-section of specimen on the normalized creep rupture strain, ε_R/D.

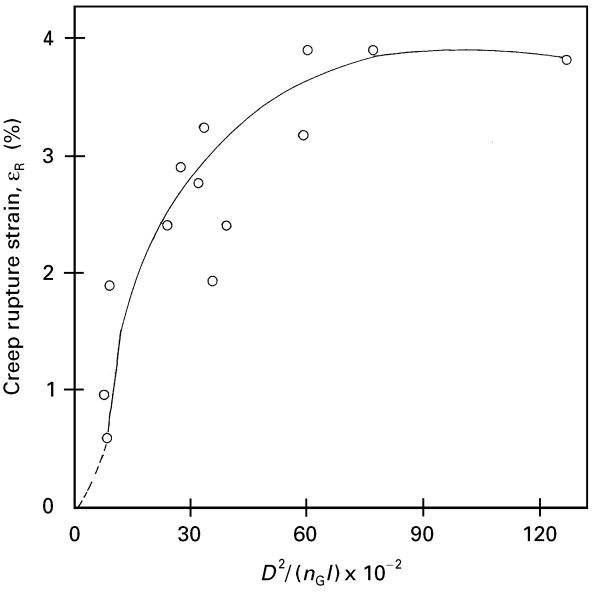

Figure 6 Creep rupture strain continuously improves with increasing $D^2/(n_G l)$ up to a certain value of this ratio.

effect on ductility. As can be seen in Fig. 6 a balance is reached when the ratio between cross-sectional area, i.e. D^2, and the $n_G l$ product becomes greater than 50×10^{-2} μm^{-1}.

As the diameters of the specimens were varied the creep rupture life was evaluated using the so-called normalized creep rupture life, t_R/D, versus the specimen gauge section diameter, D (Fig. 7), which indicated that there was no unique relationship between t_R/D and the section size. Fig. 8a illustrates the effect of the ratio of cavity size to grain size, d_C/d, on the creep rupture life, where $d_C = f_C/(\pi N_C)^{1/2}$ and f_C is the cavity volume fraction and N_C the cavity density (or the

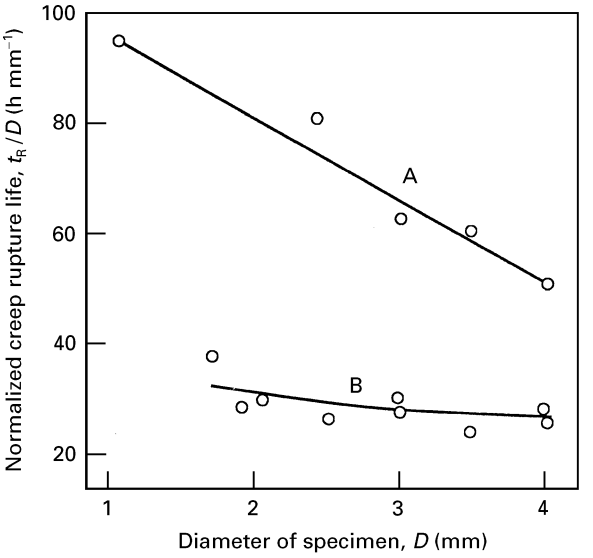

Figure 7 Effect of section size, D, on the normalized creep rupture life, t_R/D.

number of cavity particles per cross-section). This figure indicates the rapid improvement of the creep rupture life with the reducing cavity to grain size ratio. The plot of the t_R against d_C/D, as seen in Fig. 8b, shows a similar behaviour to that in Fig. 8a, indicating that the grain size, d, and the specimen diameter, D, have similar effects on t_R, whereas the cavity size, d_C, has the opposite effect on t_R. Therefore, normalizing of the d_C/d ratio by D [or $d_C/(dD)$] and plotting t_R against this ratio seems to give a better correlation with reduced scatter in the data, as seen in Fig. 8c. From the similarity of the curves in Fig. 8a and b it is concluded that the effects of grain size and thin-section size are sufficiently similar to indicate that related mechanisms may be involved. In Fig. 8c there is a critical value of the $(d_C/d)/D$ ratio ($\approx 100 \times 10^{-8}$ μm^{-1}) below which the creep rupture life increases sharply. The $t_R \propto 1/[(d_C/d)/D]$ relationship in Fig. 8c can be rearranged as follows

$$t_R \propto [(Dd)/d_C] \times (D/D)$$

As defined previously, $D/d = n_G$ (the number of grains per gauge cross-section of specimen) yields

$$t_R \propto D^2/(n_G d_C) \quad (3)$$

Equation 3 indicates that the creep rupture life of the alloy improves by increasing the diameter of the test-piece and by reducing the number of grains, n_G, in the gauge cross-section and cavity size, d_C. As in the case of the rupture ductility, a large cross-sectional area, i.e. D^2, leads to a higher t_R as a consequence of the thin-section size effect, whereas the number of grain boundaries meeting the specimen surface has the opposite effect, and a balance is reached when the ratio between cross-sectional area, i.e. D^2, and the $n_G d_C$ product becomes greater than two. It appears from Equations 2 and 3 that both the creep rupture life and rupture strain are affected by the same common factor, i.e. D^2/n_G.

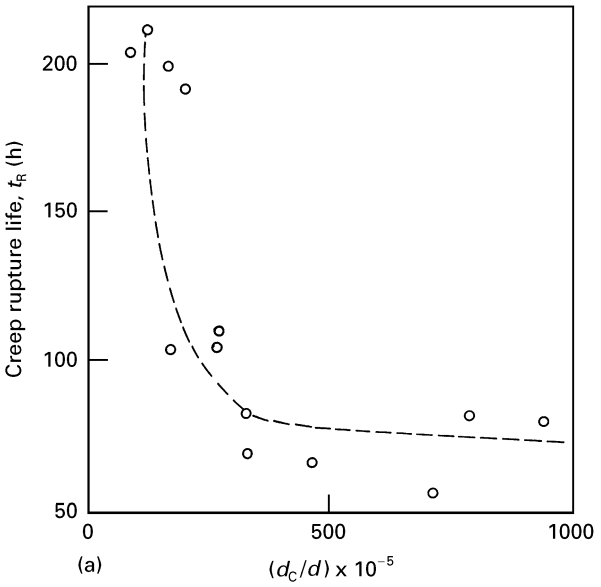

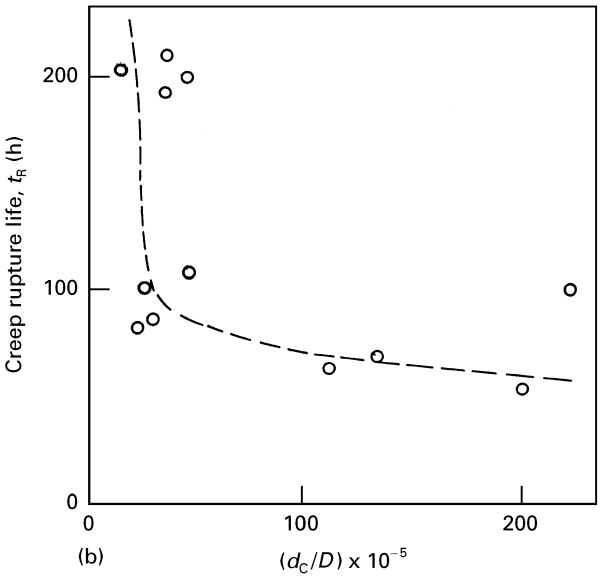

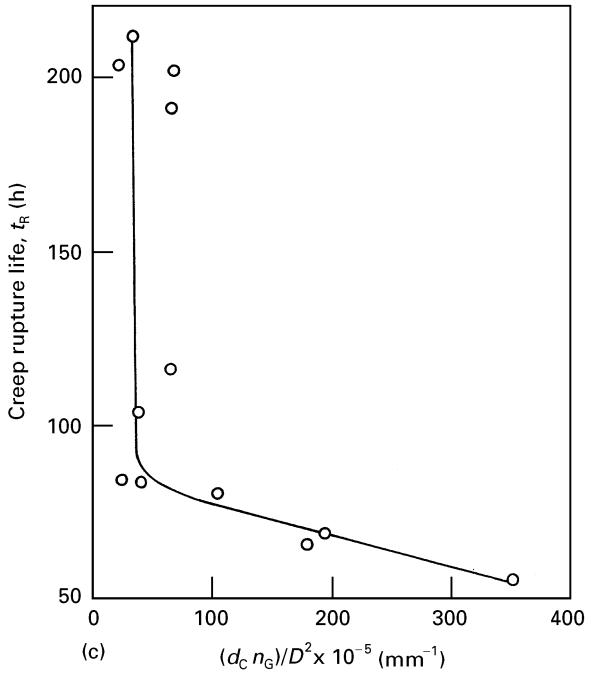

Figure 8 Effects of cavity size, d_C, grain size, d, and thin-section size, D, on the creep rupture life, t_R: (a) t_R versus d_C/d; (b) t_R versus d_C/D; and (c) the combined effects of d_C, d and D, i.e. $d_C/(dD)$ or equivalently $(n_G d_C)/D^2$, on the creep rupture life.

4. Discussion

4.1. Cavity growth mechanism

Needleman and Rice [9] showed that the coupling between diffusion and creep can be expressed in terms of a stress and temperature dependent "material length constant" or characteristic diffusion length

$$\Lambda = [(\delta_B D_B \Omega \sigma_\infty)/(kT\dot{\varepsilon}_\infty)]^{1/3} \quad (4)$$

where Λ is the diffusive coupling length (or material length scale), δ_B the grain boundary (GB) thickness, D_B the GB diffusion coefficient ($m^2 s^{-1}$), Ω the atomic volume (m^3), k the Boltzmann constant ($1.38 \times 10^{-23} J K^{-1}$), T the absolute temperature, σ_∞ the applied stress, and $\dot{\varepsilon}_\infty$ the remote creep rate (or the minimum creep rate, $\dot{\varepsilon}_m$). The contribution of dislocation creep to cavity growth is shown to be negligible when $\Lambda > L$, where L is the cavity spacing [$L = 0.5/(N_C)^{1/2}$, where N_C is the number of cavities per cross-section of the specimen]. Significant interaction occurs when $\Lambda < L$.

Edward and Ashby [10] obtained the size of the diffusional zone by the dimensionless parameter, P^*

$$P^* = (1/10)(4\Lambda^3/L^3)^{2/n} \quad (5)$$

This parameter is also useful for determining which cavity growth mechanism dominates the creep life. The quantity P^* is temperature dependent (directly and through D_B); and it depends inversely on the strain rate, $\dot{\varepsilon}_m$. It is P^* that controls the size of the diffusion zone. They observed [10] that for $P^* \geqslant 1$, i.e. for large values of parameter, Λ or for small cavity spacing, there is a negligible contribution of creep flow to cavity growth, and the rupture process is controlled by GB diffusion; for $P^* \leq 10^{-3}$, they suggested that GB diffusion is negligible and rupture is controlled, essentially, by creep flow alone. If P^* lies in the range $10^{-3} \leq P^* \leq 1$, coupling of power law cavity growth and diffusional relaxation may be significant [10].

Using the following material constant [8] for MAR-M 002 alloy the values of Λ and P^* were calculated for various $\dot{\varepsilon}_m$ (or $\dot{\varepsilon}_\infty$) and L values observed in the present investigation for this alloy

$\delta_{OB} D_{OB} = 2.8 \times 10^{-15} m^3 s^{-1}$
$\Omega = 1.1 \times 10^{-29} m^3$
$Q_B = 115 kJ mol^{-1}$
$n = 4$ (stress exponent for power law creep)

where $\delta_{OB} D_{OB}$ is the pre-exponential term for GB diffusion constant and Q_B the activation energy for GB diffusion. Note that $\delta_B D_B$ in Equation 4 was calculated using the following Arrhenius type equation [11]

$$\delta_B D_B = \delta_{OB} D_{OB} \exp[-Q_B/(RT)] \quad (6)$$

where R is the gas constant ($8.31 J mol^{-1} K^{-1}$) and T the temperature.

At present creep conditions ($T = 1173$ K, $\sigma_\infty = 300$ MPa) depending on the observed values of L and $\dot{\varepsilon}_m$ (or $\dot{\varepsilon}_\infty$) the following values of Λ and P^* are determined: $\Lambda \approx 180$–$340\ \mu m > L \approx 10$–$25\ \mu m$; $P^* \approx 10$–$50 > 1$. These numerical calculations indicate that there is a negligible contribution of creep flow to cavity growth, and so the creep rupture process in MAR-M 0 0 2 at the present creep conditions (1173 K, 300 MPa) is controlled by the GB diffusion mechanism, despite the fact that the diameters of the specimens and microstructure vary widely.

It is generally believed that intergranular cavities (and/or microcracks) are nucleated at geometrical or structural irregularities, such as hard particles and triple grain junctions on grain boundaries, where stress concentrations can develop. Cavity or crack formation along grain boundaries in creeping alloys requires both the presence of GB particles and grain boundary sliding (GBS), which are prerequisites for intergranular cavitation [12]. The stress concentrations required for the nucleation of cavitation must be the result of incompatibilities produced by GBS [12]. Argon and coworkers [12, 13] have investigated the stress concentrations at GB particles and grain junctions. They assumed that the GB particles carry the full applied load because the clean portions of the boundaries are assumed to slide freely. The average stress, σ_P, necessary to cause fracture at particle interfaces should therefore be of the order of [14]

$$\sigma_P \cong \sigma_{12}^{\infty}(a_0/\lambda)^2 \tag{7}$$

where σ_{12}^{∞} is the applied resolved shear stress on the boundary, a_0 is the carbide particle size $[a_0 = f_0/(\pi N_0)^{1/2}]$, f_0 is the volume fraction of carbides, N_0 is the number of carbide particles per cross-section and λ is the carbide particle spacing $[\lambda = 0.5/(N_0)^{1/2}]$. $(a_0/\lambda)^2$ is the area fractions of particles in the boundary. Equation 7 has been used to predict the stress necessary $[\sigma_P \propto (a_0/\lambda)^2]$ to cause failure. The variation of this stress is plotted against d_C/d, and the result is shown in Fig. 9. There is a similarity in shape between Figs 8a and 9. Fig. 9 predicts that below a critical value ($\sim 20 \times 10^{-4}$) of the d_C/d ratio in Fig. 8a, the stress necessary to cause failure (or the stress necessary for cavity nucleation) at particle interfaces increases rapidly with decreasing d_C/d ratio, which makes the creep rupture life longer with reducing d_C/d ratio. Therefore, it is concluded that the variation of the creep rupture life as a function of d_C/d [or of $(d_C/d)/D$] is caused as a result of variation of the stress necessary to cause fracture on the GB carbide particles. According to stress calculated by Lau and Argon [15] the main contributions to the high stress concentrations at particles come from the term $(\lambda/a_0)^2$ (see Equation 7) or from the reciprocal of the area fraction of the boundary covered with particles. This geometrical effect [12] is consistent with the stress concentration factor calculated by Smith and Barnby [16]. However, Argon [12] has objected to other Smith–Barnby models [16] that are based on linear elastic approximations utilizing dislocation pile-ups, on the ground that the matrix can undergo plastic deformation during creep.

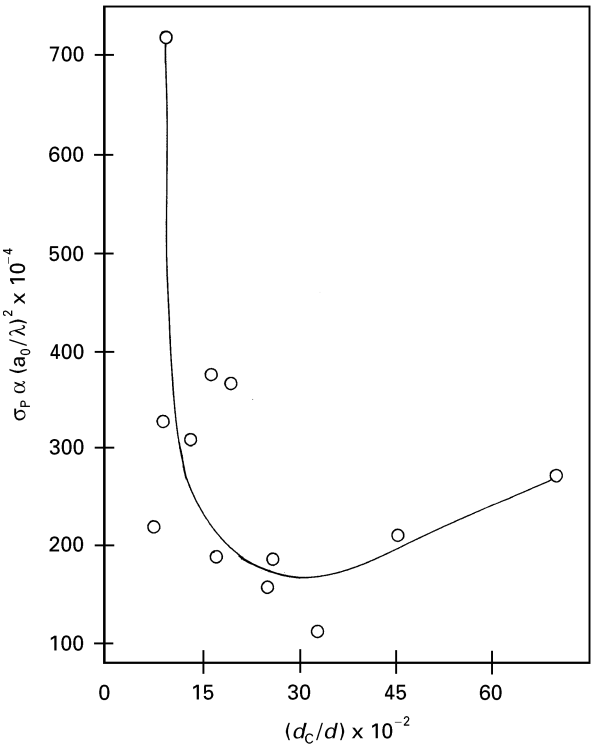

Figure 9 Correlation between the stress required to cause failure, σ_P and the d_C/d ratio (a trend similar to that in Fig. 8a is shown).

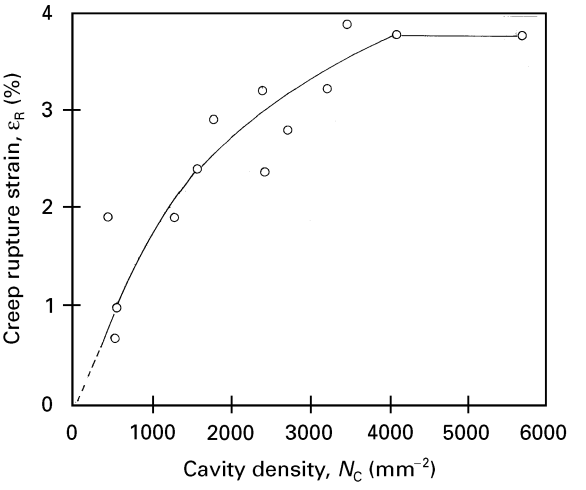

Figure 10 A plot of cavity density, N_C, versus the creep rupture strain.

A plot of creep rupture ductility against cavity density, N_C, is shown in Fig. 10. This figure indicates that increasing the cavity density rapidly improves the creep ductility up to a limiting value of the cavity density. As can be suspected from the similarity in shapes of Figs 6 and 10, there must also be a correlation between the cavity density and $D^2/(n_G l)$, as seen in Fig. 11. This plot gives good linear correlation between N_C and $D^2/(n_G l)$; increasing the diameter of the testpiece or decreasing the number of grains in the gauge section linearly increases the cavity density, which in turn improves the creep rupture ductility. We may give the following explanation for the dependence of cavity density, N_C, on the strain, ε_R, and the parameter $D^2/(n_G l)$. Reduction in n_G or an increase in

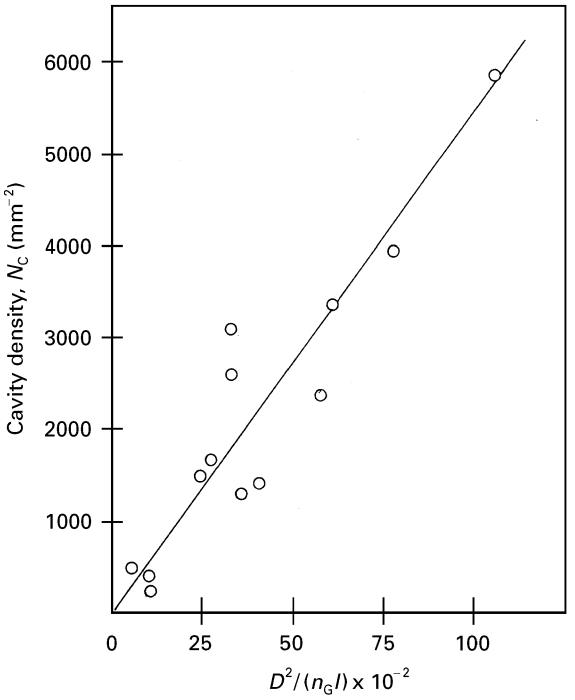

Figure 11 Plot to the good linear correlation between N_C and $D^2/(n_G l)$.

D lead to an increase in grain size, d, because $n_G = D/d$, which in turn decreases the grain boundary area for cavitation. As a result of this decreased grain boundary area the cavity density increases with increasing D or decreasing n_G because N_C varies with the applied stress and strain, ε (i.e. $N_C/\varepsilon \propto \sigma^n$) [17] for a constant microstructure and a "normal" (or "thick") specimen.

4.2. Effects of grain boundary sliding and creep crack growth

Cavity nucleation occurs as a consequence of stress concentrations developed at, for example, GB carbide particles, where GBS is inhibited by these particles so that the rate of sliding depends on the rate at which diffusion or plastic strain accommodation can occur through or around particles. This inhibition of sliding leads to local stress concentrations, which are dependent on the spacing, λ, and the size, a_0, of the GB carbide particles (i.e. the reciprocal of Equation 7). It has been suggested occasionally that GBS and diffusional creep are independent deformation processes. If diffusion is the only dominant mechanism (as in the present case) of accommodating the compatibilities caused by GBS, diffusional flow and GBS are not independent. As pointed out by Raj and Ashby [18], diffusion and GBS are coupled, and the resulting creep deformation in the present work can be correctly described either as "diffusional creep" or as "GBS with diffusional accommodation". Therefore, GBS is an integral part of diffusional creep, and without GBS no incompatibilities can develop, and no diffusional creep is possible [18]. Cane [19] has observed, for small strains, a linear relationship between the cavity nucleation rate, $\dot{N}$, and the strain rate, $\dot{\varepsilon}$, that is expected from the stochastic sliding model of grain boundaries, where repeated trials are necessary to bring a cavity through the subcritical range into a super critical size [12]. Because GBS must be synchronized with matrix creep for reasons of compatibility, a proportionality between $\dot{N}$ and $\dot{\varepsilon}$ and between N (cavity density) and ε (strain) must follow [12], which is consistent with present observations (see Fig. 10) for small strains, whereas for large strains there is a saturation effect.

GBS occurs by the relative motion of neighbouring grains along their common boundaries. GBS can be considered as the primary deformation mechanism, and diffusion creep may be considered to be an accommodating process. Therefore, it will be helpful to determine GBS in order to gain some understanding of the combined effects of grain structure, cavitation process, and as well as the thin-section size. To determine the strain, ε_{gb}, caused by GBS the following expression may be used [20]

$$\varepsilon_{gb} = (1 + \varepsilon) n_L \bar{u}_L \tag{8}$$

Where n_L is the number of grains per unit length of longitudinal line, measured after creep, $\bar{u}_L$ is the mean longitudinal GBS component measured along a line parallel to the tensile axis and ε is the total creep strain. Because the measurements of GBS were outside the scope of this investigation we did not measure $\bar{u}_L$. However, assuming the relative variation of the vector component $\bar{u}_L$ with respect to n_L and $(1 + \varepsilon)$ constant terms then we rewrite Equation 8 as follows

$$\varepsilon_{gb} \propto n_G (1 + \varepsilon_R) \tag{9}$$

Note that here ε_{gb} is the strain due to GBS at fracture. Also, frequently, it holds that [21]

$$(\varepsilon_{gb}/\varepsilon) \cong (\dot{\varepsilon}_{gb}/\dot{\varepsilon}) \tag{10}$$

Where $\dot{\varepsilon}_{gb}$ is the creep rate component due to GBS and $\dot{\varepsilon}$ is the creep rate. Rewriting Equation 10 and inserting the value of ε_{gb} into Equation 8 gives

$$(\dot{\varepsilon}_{gb}/\dot{\varepsilon}) \cong [(1 + \varepsilon) n_G \bar{u}_L]/\varepsilon \tag{11}$$

or

$$(\dot{\varepsilon}_{gb}/\dot{\varepsilon}) \cong (1 + 1/\varepsilon) n_G \bar{u}_L$$

rearranging this

$$\dot{\varepsilon}_{gb} \cong n_G (1 + 1/\varepsilon) \bar{u}_L \dot{\varepsilon}$$

Assuming again the relative variation of the product $(\bar{u}_L \dot{\varepsilon})$ is similar to the terms n_G and $(1 + 1/\varepsilon)$ then we may write that the GBS rate, $\dot{\varepsilon}_{gb}$, is proportional to the parameter $n_G [1 + 1/\varepsilon_R]$, i.e.

$$\dot{\varepsilon}_{gb} \propto n_G (1 + 1/\varepsilon_R) \tag{12}$$

Here $\dot{\varepsilon}_{gb}$ is the measure of the GBS rate at fracture. Therefore, we may use Equations 9 and 12 to measure the relative variations of the strain due to GBS and to the rate of GBS.

The presence of carbide particles in the grain boundaries gives rise to sufficient stress concentration to nucleate cavities along the grain boundaries by blocking GBS [see the plot of d_C/d versus $(\lambda/a_0)^2$ in Fig. 12]. In this study the importance of GBS on the thin-section size dependent creep strength (i.e. t_R, ε_R) of the CC MAR-M 002 is demonstrated. Fig. 13

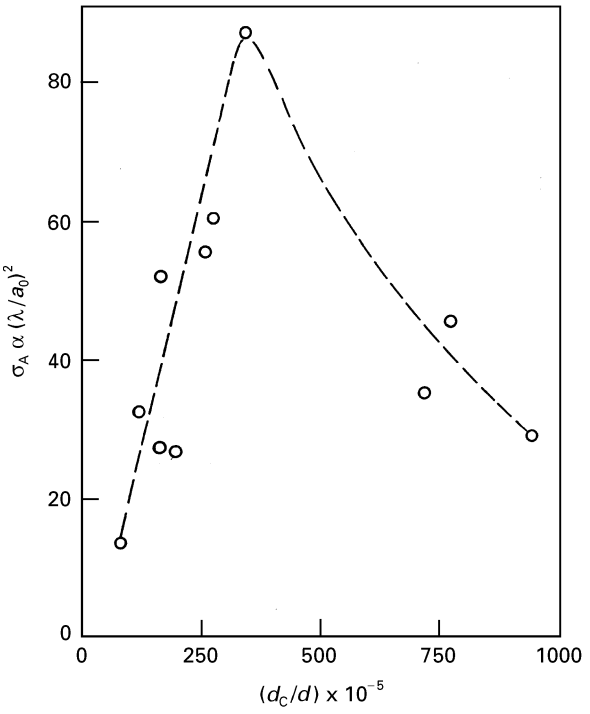

Figure 12 Variation of stress concentration with d_C/d.

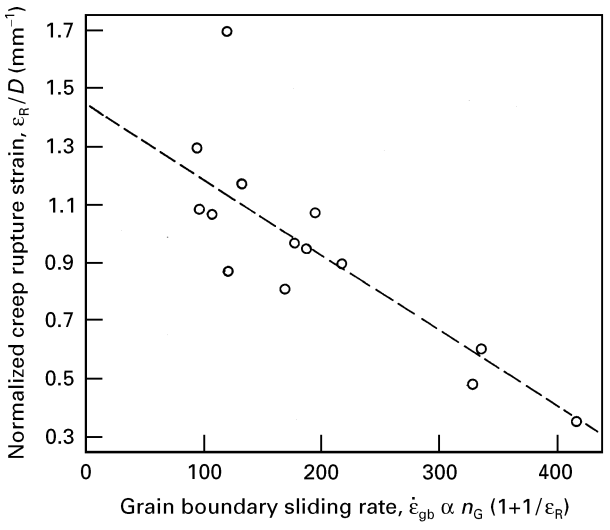

Figure 13 Inverse linear correlation between ε_R/D and the GBS rate, $\dot{\varepsilon}_{gb}$.

indicates that the thin-section size dependent creep rupture strain, ε_R/D, is directly controlled by the GBS rate, $\dot{\varepsilon}_{gb}$; reducing the GBS rate improves the thin-section size dependent rupture ductility. Therefore, reducing the l/d ratio, i.e. increasing the grain size, decreases the GBS rate, and in turn improves the ductility of the material (see Fig. 4). The GBS rate is also plotted (Fig. 14) against the $D^2/(n_G l)$ ratio that controls the rupture ductility (see Fig. 6). In conclusion, increasing the $D^2/(n_G l)$ ratio reduces the GBS rate, and as a result the rupture ductility improves, especially above the critical value ($\sim 50 \times 10^2$) of the $D^2/(n_G l)$ ratio, which also corresponds to a critical value of $\dot{\varepsilon}_{gb}$. Fig. 15 shows a plot of the strain due to the GBS contribution, ε_{gb}, against $D^2/(n_G l)$; there is a maximum value of ε_{gb} at the critical value of the

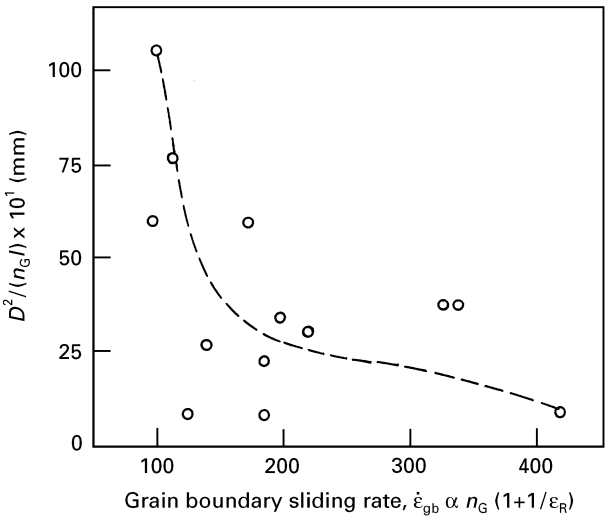

Figure 14 The dependence of the GBS rate, $\dot{\varepsilon}_{gb}$, on $D^2/(n_G l)$.

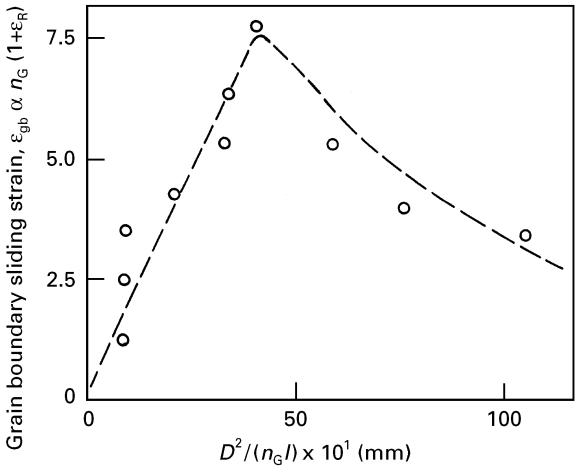

Figure 15 Plot showing the maximum value of the strain due to GBS, ε_{gb}, at a critical value of the $D^2/(n_G l)$ ratio.

ratio ($\sim 50 \times 10^2$) below which the rupture ductility, ε_R, increases rapidly as in the case of ε_{gb}. Above the critical value of this ratio ε_{gb} decreases rather rapidly. Comparison of Fig. 15 with Fig. 6 indicates the contribution of strain due to GBS, ε_{gb}, to the total strain, ε_R, is dominant below the ($\sim 50 \times 10^2$); ratio and above the critical value of the ratio it is believed that the fall of strain due to GBS, ε_{gb}, is balanced by the increasing contribution of strain due to matrix deformation, ε_g because ε_R hardly varies above the critical value of the ratio. (It is assumed that ε_R consists of ε_{gb} and ε_g components and no interactions between these components.) Therefore, the initial rapid improvement of ductility, ε_R, with increasing $D^2/(n_G l)$ is due to the reduction in the GBS rate below a critical value. The occurrence of a maximum in ε_{gb} versus $D^2/(n_G l)$ and the increase in ε_{gb} with increasing $D^2/(n_G l)$ ratio below the critical value can be attributed to the increasing importance of GBS as a deformation process as this ratio increases. The distance travelled by dislocations across the grain and along the GB will determine the ratio of the strain resulting from GBS, ε_{gb}, to the overall creep strain, i.e. $\varepsilon_{gb}/\varepsilon_R$.

Comparing the thin-section size dependent creep rupture life, t_R/D, with the GBS rate, $\dot{\varepsilon}_{gb}$, (Fig. 16) it is clear that a reduction in $\dot{\varepsilon}_{gb}$ below a critical value results in a large increase in t_R/D, and that above this critical value t_R/D is almost constant and has a rather low value. Therefore, this correlation (Fig. 16) shows that when fracture occurs by the GB diffusion process the GBS rate is an important factor governing the creep rupture life of the material. Fig. 17 shows the dependence of the stress necessary to cause failure, $\sigma_P \propto (a_0/\lambda)^2$, on the GBS rate, $\dot{\varepsilon}_{gb}$. Again, this correlation indicates that reducing the GBS rate first increases σ_P slowly, and below that critical value of $\dot{\varepsilon}_{gb}$, σ_P increases sharply, which indicates that the material becomes much stronger below a critical value of $\dot{\varepsilon}_{gb}$. In other words, increasing the area fraction, $(a_0/\lambda)^2$, of GB carbide particles, especially above a critical value, makes the alloy much stronger, and as a result the GBS rate is reduced below a critical value and the thin-section size dependent creep rupture life, t_R/D, is extended appreciably.

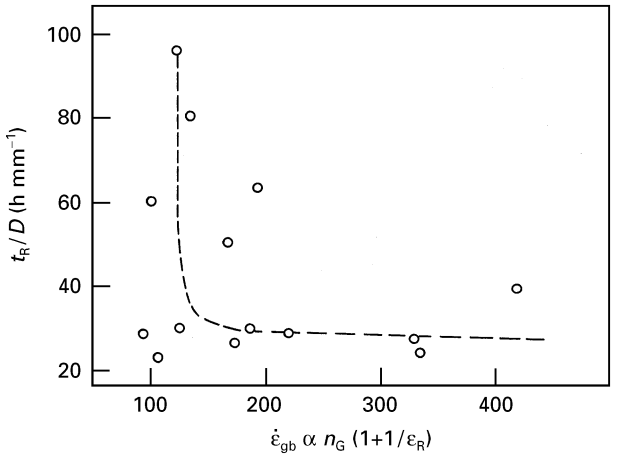

Figure 16 The effect of the GBS rate, $\dot{\varepsilon}_{gb}$, on the thin-section size dependent creep rupture life, t_R/D.

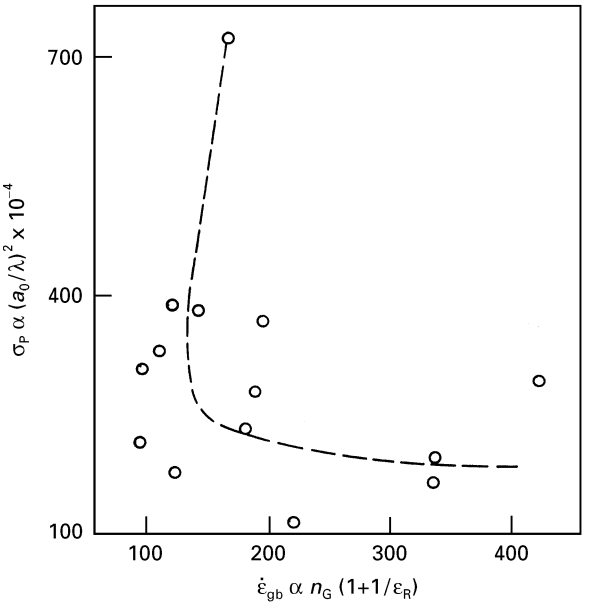

Figure 17 The dependence of the stress, σ_P, required to cause failure on the GBS rate, $\dot{\varepsilon}_{gb}$.

Because time-dependent crack growth at high temperatures is mostly due to creep, there have been several models developed relating creep crack growth (CCG) to creep deformation rates. Almost all models assume some criteria for CCG, such as critical strain, critical displacement, or time for fracture of a critical size ligament ahead of the crack tip [22]. As pointed out by Sadananda and Shahinian [22], it is likely that, in most alloys, CCG occurs by an integrally coupled diffusion-GBS deformation mechanism. Under the creep conditions where GBS is dominant, as in the present study, the CCG rate is proportional to d^{-m} (where m is a constant) in a similar way to the minimum creep rate, $\dot{\varepsilon}_m$ [23]. Therefore, the creep rupture strength (i.e. t_R, ε_R) improves when the grain size increases, which is consistent with present observations, i.e. Figs 4, 6 and 8c. In other words, grain refinement (or, equivalently, increasing the number of grains) reduces creep rupture life and creep rupture ductility, which are consistent with the previous experimental and theoretical findings that the CCG rate of superalloys, such as IN-792, IN-100, accelerates with grain refinement [23]. Sadananda and Shahinian [22] developed a model to relate the CCG rate to the GBS rate, $\dot{\varepsilon}_{gb}$, where the CCG rate was dictated by the GBS rate

$$\text{CCG rate} = (2d\,\dot{\varepsilon}_{gb}) \tag{13}$$

Using Equation 12, Equation 13 can be rewritten as

$$\text{CCG rate} = 2d[n_G(1 + 1/\varepsilon_R)] \tag{14}$$

Fig. 18 shows the variation of CCG rate with grain size. In this figure the CCG rate is more or less the same with reducing grain size until a critical value is reached, and below that critical value of grain size the CCG rate accelerates rapidly, which is consistent with previous findings [23]. Floreen [24] studied the influence of grain size, d, on the stress intensity factor, K, and found that increasing the grain size markedly improved crack propagation resistance, K, of IN-792.

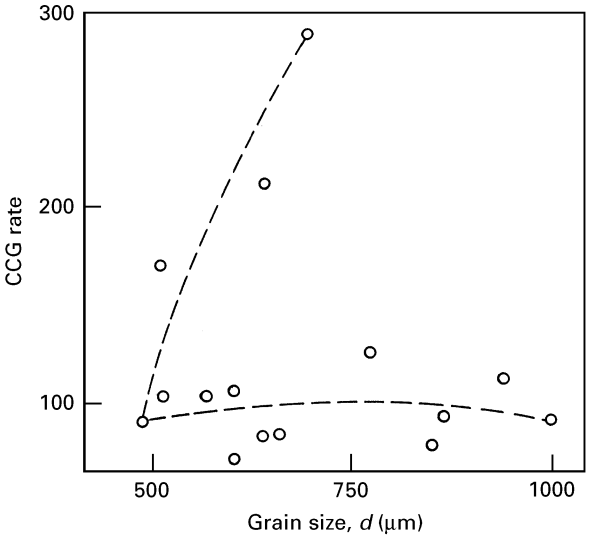

Figure 18 The CCG rate versus grain size.

The strong influence of grain size, as in the present case, on the creep crack propagation behaviour of IN-792 was explained by the critical strain, ε_C, model of Floreen and Kane [25]. In this model, intergranular creep fracture propagates when the local strain, ε_l, ahead of the crack tip reaches a critical value, i.e. $\varepsilon_l \rightarrow \varepsilon_C$. This value of critical strain, ε_C, was suggested [25] to be related to the microstructure of the GB, i.e. to the distribution of carbides, wave form, segregation, denuded zones, etc., as well as to the internal structure of the grains, i.e. the γ' morphology, etc.

Fig. 19 illustrates the effect of grain size on the cavity size. This figure suggests that there is a critical grain size below which the crack size increases sharply, and that above the critical grain size the crack size is small and increases slowly with reducing grain size. The plot of cavity density, N_C, against grain size, d, also shows the existence of this critical grain size (see Fig. 2c) below which N_C also increases sharply. Fig. 20 illustrates the effect of cavity size, d_C, on the thin-section dependent creep rupture life, t_R/D, indicating the existence of a critical value of cavity size; below the critical d_C value t_R/D increases sharply. Comparing Figs 19 and 20, there is a critical value of grain size below which the crack size increases, and as a result t_R/D deteriorates.

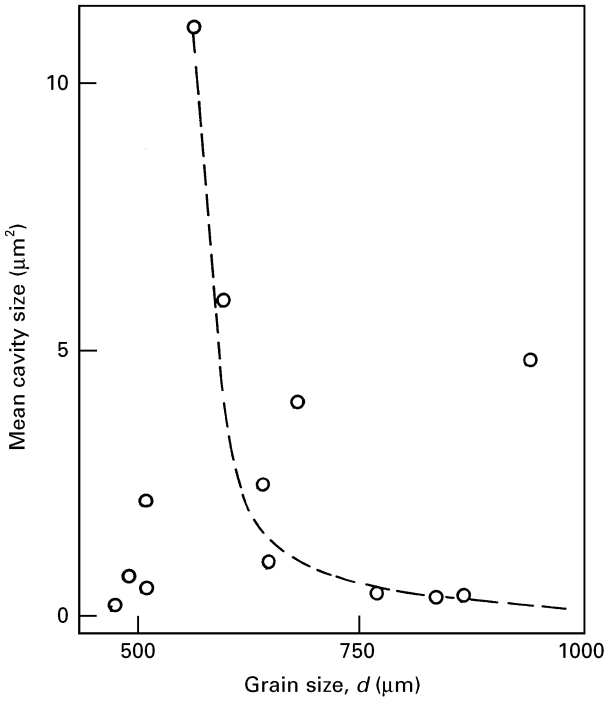

Figure 19 Plot to show the effect of grain size on cavity size (suggests the existence of a critical grain size below which there is a sharp increase in the crack size).

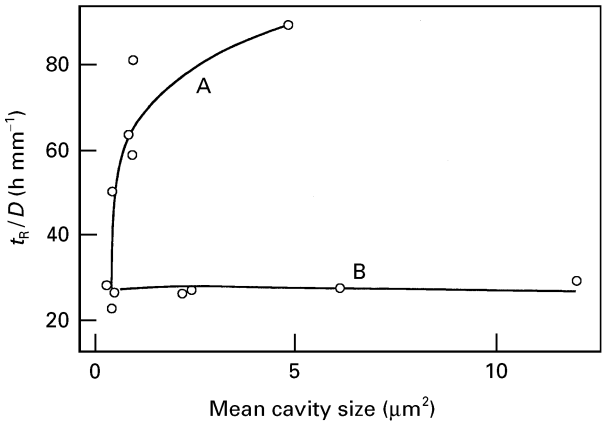

Figure 20 t_R/D versus cavity size.

5. Conclusions

The grain size is one of the most important factors in determining the properties of creep because of the role played by grain boundaries during deformation. The influence of grain size on mechanical properties may either act as obstacles to dislocation slip (a strengthening effect) or provide a positive contribution to the deformation of the material (a softening effect) [23], depending on the presence of carbide particles and their densities [26]. A drastic increase in tensile ductility can be achieved as a result of grain refinement [23] at relatively low temperatures, delaying crack nucleation and increasing ductility [23]. Whereas in the present studies, the creep rupture strain improves by increasing the grain size (Fig. 4), by reducing the number of grains (Fig. 6). On the other hand, the number of grains, n_G, or the grain size, d, have beneficial effects on t_R, as in the case of ductility. From Equations 2 and 3 it can be concluded that the reduction in the D^2/n_G ratio has the same detrimental effect on the creep rupture life, t_R, and on ductility, ε_R.

When n_G approaches unity ($n_G \rightarrow 1$) creep rupture strain can be maximized, as suspected from examination of Fig. 5. Therefore, for a turbine blade with a certain thin-section size, the creep rupture strain can be improved dramatically using a single crystal ($n_G = 1$) alloy and reducing the intercavity spacing, l (or equivalently increasing the cavity density, N_C), through suitable heat treatment and reducing porosities [27]. However, it is difficult to change the mean intercavity spacing by more than a factor of five or so [28]. An investigation of the single crystal (SC) MAR-M 002 by the present author [27] has shown that there is a good correlation between the creep rupture strain and the D^2/l ratio, which confirms the present result for CC MAR-M 002.

As Fig. 11 suggests, by extrapolating the $D^2/(n_G l)$ ratio to zero the cavity density, N_C, also approaches zero. This suggests that by reducing the $D^2/(n_G l)$ ratio to zero the creep rupture strain approaches zero as well, as indicated by the dotted line in Fig. 6. Therefore, another possibility for improving the creep rupture ductility is to increase the cavity density (Fig. 10). Because the cavitation process begins as soon as the creep deformation starts, and cavity nucleation is continuous and stochastic in nature throughout the creep life [13] the creep strain is also expected to be controlled by cavity nucleation through the creep life in the present study. However, the cavity density is not an independent parameter, but is controlled by the $D^2/(n_G l)$ ratio (Fig. 11). Therefore, increasing the $D^2/(n_G l)$ ratio linearly increases the cavity density, which in turn improves the creep rupture ductility.

It is demonstrated that an appreciable improvement in the thin-section size dependent creep rupture life, t_R/D, can be made by reducing the crack size below a critical value through increasing the grain size above a critical value; whereas below the critical grain size value the crack size and the CCG rate sharply increase, and in turn t_R/D deteriorates. Therefore, deterioration of the rupture life above a certain value of $d_C/(dD)$ [or, equivalently, the $(n_G d_C)/D^2$ ratio] is due to the rapid increasing of crack size with reducing grain size below a critical value. Let us return to Fig. 12, which shows the variation of the reciprocal of the area fraction of grain boundaries covered with carbide particles [i.e. $(\lambda/a_0)^2$ is proportional to the stress intensity factor; see Equation 7] as a function of the cavity size to grain size ratio, d_C/d, this indicates the definite relationship between the GB carbide particle parameter, $(\lambda/a_0)^2$ and the d_C/d ratio. Fig. 12 further indicates the existence of a critical value between the grain size and cavity size at which the stress intensity is highest. Comparison of Figs 12 and 8a indicates that at this critical value of d_C/d the creep rupture life is shortest and is associated with the highest stress intensity; furthermore, t_R is longest at the lowest value of d_C/d, which corresponds to the lowest stress intensity, $(\lambda/a_0)^2$.

The following conclusions can therefore be made.

1. It is predicted that the creep rupture process is controlled by the GB diffusion mechanism.

2. The creep rupture ductility, ε_R, is controlled by $\varepsilon_R \propto D^2/(n_G l)$. The influence of the specimen surface, D, in improving the creep ductility is twice as effective as the GB interface, n_G.

3. The creep rupture ductility is also controlled by the cavity density in a similar way as the $D^2/(n_G l)$ ratio. Linear correlation between the cavity density and this ratio indicates that the cavity density is directly controlled by $D^2/(n_G l)$.

4. The creep rupture life can be dramatically improved below a critical value ($\sim 100 \times 10^{-8}\ \mu m^{-1}$) of the reduced $(d_C/d)/D$ [or $(d_C n_G)/D^2$ ratio].

5. It is predicted that variation of the creep rupture life as a function of the $(d_C/d)/D$ ratio [or, equivalently, the $(d_C n_G)/D^2$, ratio] is caused by variation of stress concentration created by the GB carbide particles.

6. Thin-section size dependent creep rupture ductility, ε_R/D, is directly controlled by the GBS rate, $\dot{\varepsilon}_{gb}$; reducing $\dot{\varepsilon}_{gb}$ linearly increases the ε_R/D ratio.

7. The thin-section size dependent creep rupture life, t_R/D, is also controlled by the GBS rate, $\dot{\varepsilon}_{gb}$; a large improvement in t_R/D can be made by reducing $\dot{\varepsilon}_{gb}$ below a critical value. Decreasing the grain size below a critical value sharply increases the CCG rate, GBS rate and crack size; in turn the creep rupture life deteriorates. Therefore, an appreciable improvement in the creep rupture life can be made by producing an alloy with a coarse grain structure (especially one having a grain size coarser than the critical size).

References

1. E. G. RICHARDS, *J. Inst. Metals* **96** (1968) 365.
2. T. B. GIBBONS, *Metals Tech.* **8** (1981) 472.
3. M. C. PANDEY, D. M. R. TAPLIN and P. RAMA RAO, *Mater. Sci. Eng.* **A118** (1989) 33.
4. B. H. HESSLER and B. A. EWING, Metals Society, AIME TMS Spring Meeting, May 1969 (Pittsburg, PA) Paper S69-5.
5. M. R. WINSTONE, "Creep properties of unidirectionally solidified thin-section coating", National Gas Turbine Engines (NGTE) Report No. NT 1013, June (1976).
6. J. D. WITTENBERGER, *Metall. Trans.* **7A** (1976) 611.
7. D. R. MATLOCK and W. D. NIX, *ibid.* **5** (1974) 1401.
8. A. C. F. COCK and M. F. ASHBY, *Prog. Mater. Sci.* **27** (1982) 189.
9. A. NEEDLEMAN and J. R. RICE, *Acta Metall.* **28** (1980) 1315.
10. G. H. EDWARD and M. F. ASHBY, *ibid.* **27** (1979) 1505.
11. H. J. FROST and M. F. ASHBY, "Deformation mechanism maps, the plasticity and creep of metals and ceramics" (Pergamon Press, Oxford, 1982) p. 55.
12. A. S. ARGON, in "Recent advances in creep and fracture of engineering materials and structures", edited by B. Wilshire and D. R. J. Owen (Pineridge Press, Swansea, 1982) p. 1.
13. A. S. ARGON, I. W. CHEN and C. W. LAU, in Proceedings of the symposium on Creep–Fatigue–Environment Interactions, edited by R. M. Pelloux and N. S. Stoloff, New York, 18–19 September 1979 (American Institute of Mining, Metallurgical and Petroleum Engineers, Warrendale, PA, 1980) pp. 47–85.
14. H. RIEDEL, *Acta Metall.* **32** (1984) 313.
15. C. W. LAU and A. S. ARGON, in "Fracture 1977", Vol. 2, edited by D. M. R. Taplin (University of Waterloo Press, Canada, 1977) 595–601.
16. E. SMITH and J. T. BARNBY, *Met. Sci. J.* **1** (1967) 1.
17. A. BALDAN, *J. Mater. Sci.* **26** (1991) 3409.
18. R. RAJ and M. F. ASHBY, *Metall. Trans.* **2** (1971) 1113.
19. B. J. CANE, *Met. Sci. J.* **12** (1978) 102.
20. J. CADEK,"Creep in metallic materials (Elsevier, Amsterdam, 1988) p. 250.
21. T. G. LANGDON, *Phil. Mag.* **22** (1970) 689.
22. K. SADANANDA and P. SHAHINIAN, *Met. Sci. J.* **15** (1981) 425.
23. A. LASALMONIE and J. L. STRUDEL, *J. Mater. Sci.* **21** (1986) 1837.
24. S. FLOREEN, *Metal. Trans.* **6A** (1975) 1741.
25. S. FLOREEN and R. H. KANE, *ibid.* **7A** (1976) 1157.
26. A. BALDAN, *Z. Metallkde* **83** (1992) 750.
27. *Idem*, *J. Mater. Sci.* **30** (1995) 6288.
28. W. D. NIX, *Mater. Sci. Eng.* **A103** (1988) 103.

Received 21 August 1995
and accepted 17 July 1996